Supplementary Information (SI) for CrystEngComm.
This journal is © The Royal Society of Chemistry 2025

Supporting Information

The Effect of Anion Variation on the Iodine Adsorption Capacity of New Silver(I)-Dithion Coordination Polymers

Maryam Bahrani-Pour[a*], Azizolla Beheshti[a*], Tahereh Sedaghat[a], Sepideh Samiee[a], Susan Soleymani-babadi[a], Fatemeh Shakeri[a], Jan Janczak[b], and Emmanuele Parisi[c]

[a] *Department of Chemistry, Faculty of Science, Shahid Chamran University of Ahvaz, 6135783151 Ahvaz, Iran.*

[b] *Institute of Low Temperature and Structure Research, Polish Academy of Sciences, Okólna 2 str. 50-422 Wroclaw, Poland.*

[c] *Department of Applied Science and Technology, Politecnico of Turin, Corso Duca degli Abruzzi 24, I-10129 Turin, Italy.*

*E-mail: a.beheshti@scu.ac.ir

*E-mail: maryambahrani72@gmail.com

X-ray crystallography

The X-ray intensity data for selected single crystals **1**, **4-7** were collected on a four-circle κ geometry Xcalibur diffractometer with Sapphire2 area CCD detector using Mo Kα radiation (λ = 0.71073 Å) in Wrocław (Poland). Data collection, integration, scaling of the reflections, correction for Lorenz and polarisation effects and absorption corrections were performed using the *CrysAlisPro* Version 1.171.42.93a. The crystals **2** and **3** were measured on a Bruker D8 Venture TXS system equipped with a multilayer mirror monochromator and a Mo Kα rotating anode X-ray tube (λ = 0.71073 Å) in Turin (Italy). The structures were solved by the direct methods using *SHELXT*-2014/7[1] and refined using *SHELXL*-2018/3 program[2]. The hydrogen atoms were introduced in their geometrical positions and treated as rigid. Details of the crystallographic data parameters and a summary of refinement parameters are listed in Table S1. Visualisations of the structures were made with the DIAMOND 3.0 and MERCURY 3.5.1 programs.

Table S1: Single crystal data and structure refinements for **1-7**.

Compound	**(1)**	**(2)**	**(3)**	**(4)**	**(5)**	**(6)**	**(7)**
Chemical formula	$C_{17}H_{18}AgN_5S_3$	$C_{32}H_{36}AgN_8S_4$	$C_8H_9AgN_3O_3S$	$C_{32}H_{36}AgN_9O_3S_4$	$C_{18}H_{21}AgClN_5O_4S_2$	$C_{18}H_{21}AgBF_4N_5S_2$	$C_{18}H_{21}AgF_6N_5PS_2$
M_r/g mol^{-1}	496.41	826.88	335.11	830.81	578.84	566.20	624.36
crystal size/mm	0.038×0.045×0.180	0.11×0.12× 0.15	0.05×0.05× 0.10	0.034× 0.038×0.232	0.07×0.08×0.39	0.034×0.037×0.244	0.021×0.024×0.356
Radiation, λ/ Å	0.71073	1.54184	1.54184	0.71073	0.71073	0.71073	0.71073
T/K	295	293	293	100	295	295	295
crystal system	monoclinic	triclinic	orthorhombic	triclinic	triclinic	triclinic	triclinic
space group	*P2$_1$/c*	*P-1*	*Pbca*	*P-1*	*P -1*	*P-1*	*P-1*
a/Å	11.839(2)	8.4341(3)	10.4384(4)	8.2259(4)	8.7317(8)	8.6154(4)	8.9221(7)
b/Å	19.437(3)	13.2016(3)	7.9869 (4)	12.9200(10)	9.0556(8)	9.0094(4)	9.1495(9)
c/Å	8.4998(12)	16.9441(6)	25.5132(11)	16.5893(12)	14.9153(13)	14.6660(6)	15.5032(19)
α/°	90	92.035(2)	90	87.868(6)	100.097(7)	100.444(4)	99.962(9)
β/°	94.456(16)	103.887(3)	90	81.755(5)	106.306(8)	106.561(4)	105.877(9)
γ/°	90	94.377(2)	90	86.775(5)	92.910(7)	92.701(4)	92.806(7)
V/Å^3	1950.0(5)	1823.31(10)	2127.05(11)	1741.3(2)	1108.14(18)	1067.16(8)	1192.7(2)
Z	4	2	8	2	2	2	2
F(000)	1000	786	1320	852	584	568	624
D_{cal} (g·cm^{-3})	1.691	1.506	2.093	1.585	1.735	1.762	1.738
μ/mm^{-1}	1.366	7.415	17.048	0.867	1.254	1.191	1.150
T_{min} / T_{max}	0.8767 / 1.000	0.392- 1.000	0.4544- 1.000	0.9024 / 1.000	0.8768 / 1.0000	0.7785 – 1.000	0.9576 / 1.000
Total / unique / observed reflections	34705 / 4046 / 1803	25225 / 6439 / 5556	9423 / 1887 / 1459	25600 / 7546 / 4197	32495 / 5280 / 3061	23593 / 4939 / 2054	18660 / 5295 / 1541
R_{int}	0.1037	0.0552	0.0536	0.0771	0.0437	0.0648	0.0739
θ range	2.622 - 26.498	2.7- 66.9	3.465- 66.884	2.482 - 26.992	2.447 – 27.995	2.441 – 27.249	2.423 - 27.500
a, b (weighting scheme)	0.0212, 11.1939	0.0531, 0.6906	0.0434, 1.4675	0.0002, 0.000	0.0413, 0.1821	0.0452, 0.000	0.0135, 0.000
refls in refinement	4046	6439	6439	8402	5280	4939	5295
Parameters	237	438	438	446	311	283	297
Restraints	0	0	0	0	0	0	0
R [$F^2>2\sigma(F^2)$][a]	0.0983	0.0390	0.0372	0.0666	0.0486	0.0609	0.0888
wR [F^2 all refls][a]	0.1587	0.1022	0.0966	0.0806	0.1101	0.2405	0.1292
S	1.002	1.03	1.042	0.977	1.034	1.009	1.005
shift/error$_{max}$	0.001	0.000	0.000	0.001	0.001	0.001	0.002
$\Delta\rho_{max}$, $\Delta\rho_{min}$ (eÅ^{-3})	+1.4262, -0.589	+0.81, -0.79	+0.86, -0.80	+0.727, -0.766	+0.469, -0.298	+0.673, -0.468	+0.478, -0.479

[a] $R=\Sigma\ ||F_o|-|F_c||/\Sigma F_o$, $wR=\{\Sigma\ [w(F_o^2-F_c^2)^2]/\Sigma wF_o^4\}^{½}$; $w^{-1}=\sigma^2(F_o^2)+(aP)^2+bP$ where $P=(F_o^2+2F_c^2)/3$.

I_2 adsorption experiment

The 1269 ppm I_2 solution in cyclohexane was prepared by dissolving a suitable mass of solid iodine in cyclohexane. For the kinetic studies, the synthesized sulfur-based complexes were activated before use at 70°C for 24 hours. Then 5 mL of this solution was added to each of the optimized weighted samples (10 mg). The amount of iodine adsorbed by each compound was determined using UV-Vis spectroscopy over time. The adsorption capacity of sulfur-based complexes and their removal efficiency were calculated using Equations **1** and **2**.

$$Q_{eq} = \frac{(C_0 - C_{eq})V}{m} \quad \textbf{(1)}$$

$$\%\ Removal = \frac{C_0 - C_{eq}}{C_0} \times 100 \quad \textbf{(2)}$$

In the first equation, the equilibrium adsorption capacity of the adsorbents is represented by Q_{eq}(mg/g). The mass of the used adsorbent is denoted as m(g), the volume of the iodine solution as V (liter), and the initial and equilibrium concentrations (ppm) are C_0 and C_{eq}, respectively. A calibration curve of standard iodine solution at 523 nm was drawn for the calculation of the final concentrations. Four kinetics models, including the pseudo-first-order model, pseudo-second-order model, intraparticle diffusion model, and Elovich model[3–5] (Equations 3-6), were used to evaluate the results of iodine adsorption and describe the mechanism.

$$q_t = q_e(1 - e^{-k_1 t}) \quad \textbf{(3)}$$

$$q_t = \frac{{q_e}^2 k_2\, t}{(1 + q_e k_2\, t)} \quad \textbf{(4)}$$

$$q_t = x_i + k_i t^{1/2} \quad \textbf{(5)}$$

$$q_t = \frac{lna_e b_e}{b_e} + \frac{1}{b_e} lnt \quad \textbf{(6)}$$

In the adsorption process, the interactions between the adsorbate and adsorbent are described by isotherms. To analyze the interactions between the I_2 solution and sulfur-based complexes, three well-known isotherm models, the Langmuir, Freundlich, and Temkin models, were applied[6–8] (Equation 7-9). 5 mL of iodine solution with initial concentrations ranging from 1500-2400 ppm were used for the adsorption isotherm studies.

$$q_e = \frac{q_{max} C_e k_L}{(1 + C_e k_L)} \quad \textbf{(7)}$$

$$q_e = k_F C_e^{\,1/n} \quad \textbf{(8)}$$

$$q_e = B ln(A_t C_e) \quad \textbf{(9)}$$

The uptake of volatile iodine

The gravimetric method, as described in the literature references, was used to determine the amount of iodine adsorbed by the **CP-1** to **CP-7** samples. The procedure was as follows: Small beakers containing 10 mg of each sample were placed in a larger vessel with a certain amount of solid I_2. The sealed vessel was then placed in an oven at 65°C for 24 hours. After the system cooled to room temperature, the samples were weighed and the adsorbed iodine was calculated using equation 10. In this Equation, m_1 and m_2 represent the sample weight before and after iodine adsorption and α is the iodine adsorption capacity.

$$\alpha = (m_2 - m_1)/m_1 \times 100\ wt\% \quad \textbf{(10)}$$

Table S2. Selected bond distances (Å) and bond angles (°) for compounds **CP-1** to **CP-7**.

Compound	Bond distances (Å)		Bond angles (°)	
CP-1	Ag-S1	2.551(3)	S1-Ag-S3	116.1(1)
	Ag-S3	2.585(3)	S1-Ag-S2	84.9(1)
	Ag-S2	2.666(3)	S1-Ag-S2	124.0(1)
	Ag-S2	2.599(4)	S3-Ag-S2	117.8(1)
	S1-C1	1.69(1)	S3-Ag-S2	103.5(1)
	C1-N1	1.35(1)	S2-Ag-S2	110.5(1)
			Ag-S1-C1	113.5(4)
			S1-C1-N1	128.5(8)
			S1-Ag-S3	116.1(1)
			S2-Ag-S2	110.5(1)
			Ag-S1-C1	113.5(4)
			S1-C1-N1	128.5(8)
CP-2	Ag01-S3	2.5537(8)	S3-Ag01-S2	99.52(3)
	Ag01-S2	2.5786(9)	S3-Ag01-S1	110.75(3)
	Ag01-S1	2.6035(8)	S3-Ag01-S4	116.43(3)
	Ag01-S4	2.563(1)	S2-Ag01-S1	106.68(3)
	S1-C4	1.695(3)	S2-Ag01-S4	106.14(3)
	S1-Ag01	2.6035(8)	S1-Ag01-S4	115.44(3)
CP-3	Ag01-S002	2.518(1)	S002-Ag01-O007	122.5(1)
	Ag01-O007	2.373(4)	S002-Ag01-S002	108.29(4)
	Ag01-S002	2.581(1)	S002-Ag01-C00A	109.9(1)
	Ag01-C00A	2.710(5)	O007-Ag01-S002	99.5(1)
	S002-C00D	1.718(5)	O007-Ag01-C00A	107.3(2)
	S002-Ag01	2.581(1)	S002-Ag01-C00A	108.1(1)
	N003-C00C	1.473(6)	C00A-Ag01-S002	109.9(1)
	N003-C00D	1.354(5)	C00A-Ag01-S002	109.9(1)
CP-4	Ag-S1	2.559(1)	S1-Ag-S3	106.16(5)
	Ag-S3	2.579(1)	S1-Ag-S2	119.74(5)
	Ag-S2	2.565(1)	S1-Ag-S4	110.05(5)
	Ag-S4	2.604(2)	S3-Ag-S2	101.71(5)
	S1-C1	1.700(5)	S3-Ag-S4	103.30(5)
	S2-C15	1.699(5)	S2-Ag-S4	113.82(5)
CP-5	Ag-S1	2.380(1)	S1-Ag-S2	178.75(4)
	Ag-S2	2.377(1)		
CP-6	Ag1-S1	2.385(2)	S1-Ag1-S2	178.94(5)
	Ag1-S2	2.393(2)		
CP-7	Ag1-S1	2.382(3)	S1-Ag1-S2	179.8(1)
	Ag1-S2	2.391(3)		

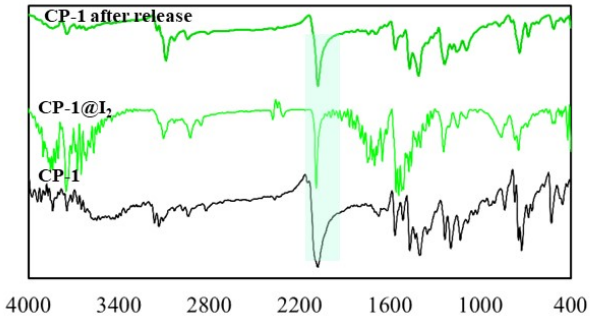
CP-1 after release
CP-1@I2
CP-1
4000
3400
2800
2200
1600
1000
400

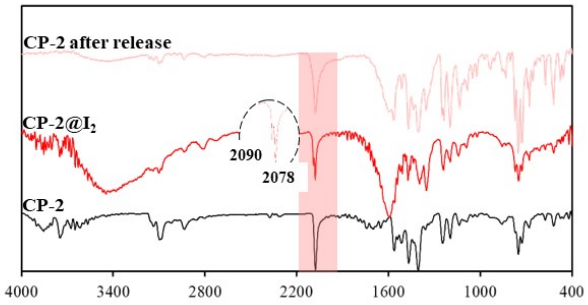
CP-2 after release
CP-2@I2
2090
2078
CP-2
4000
3400
2800
2200
1600
1000
400

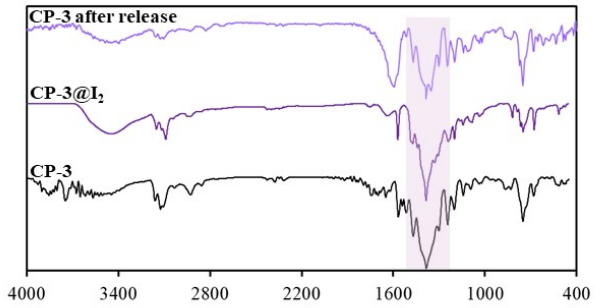
CP-3 after release
CP-3@I2
CP-3
4000
3400
2800
2200
1600
1000
400

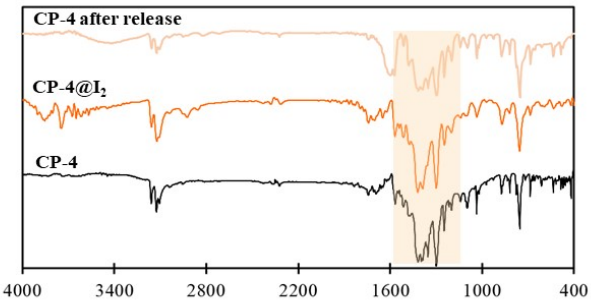
CP-4 after release
CP-4@I2
CP-4
4000
3400
2800
2200
1600
1000
400

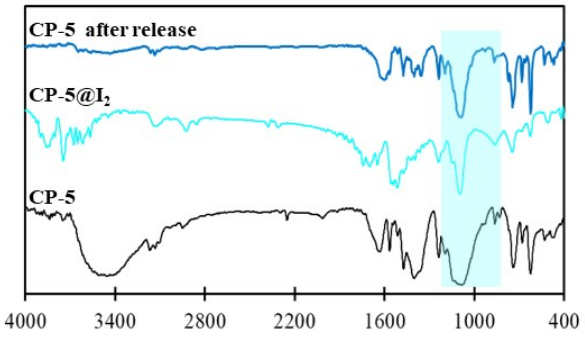
CP-5 after release
CP-5@I2
CP-5
4000
3400
2800
2200
1600
1000
400

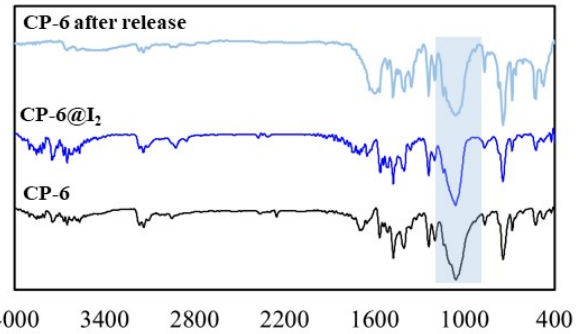
CP-6 after release
CP-6@I2
CP-6
4000
3400
2800
2200
1600
1000
400

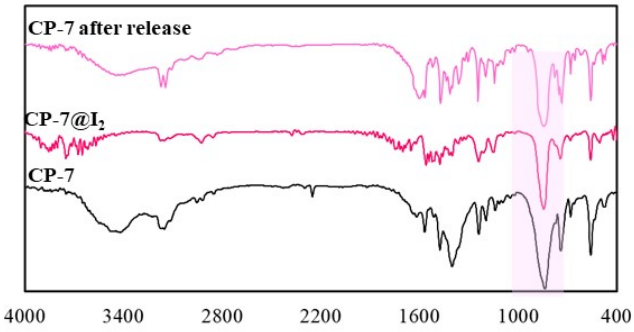
CP-7 after release
CP-7@I2
CP-7
4000
3400
2800
2200
1600
1000
400

Figure S1: The FT-IR spectra of silver(I)-dithion coordination polymers before, after iodine adsorption, and regenerated adsorbents after release of iodine.

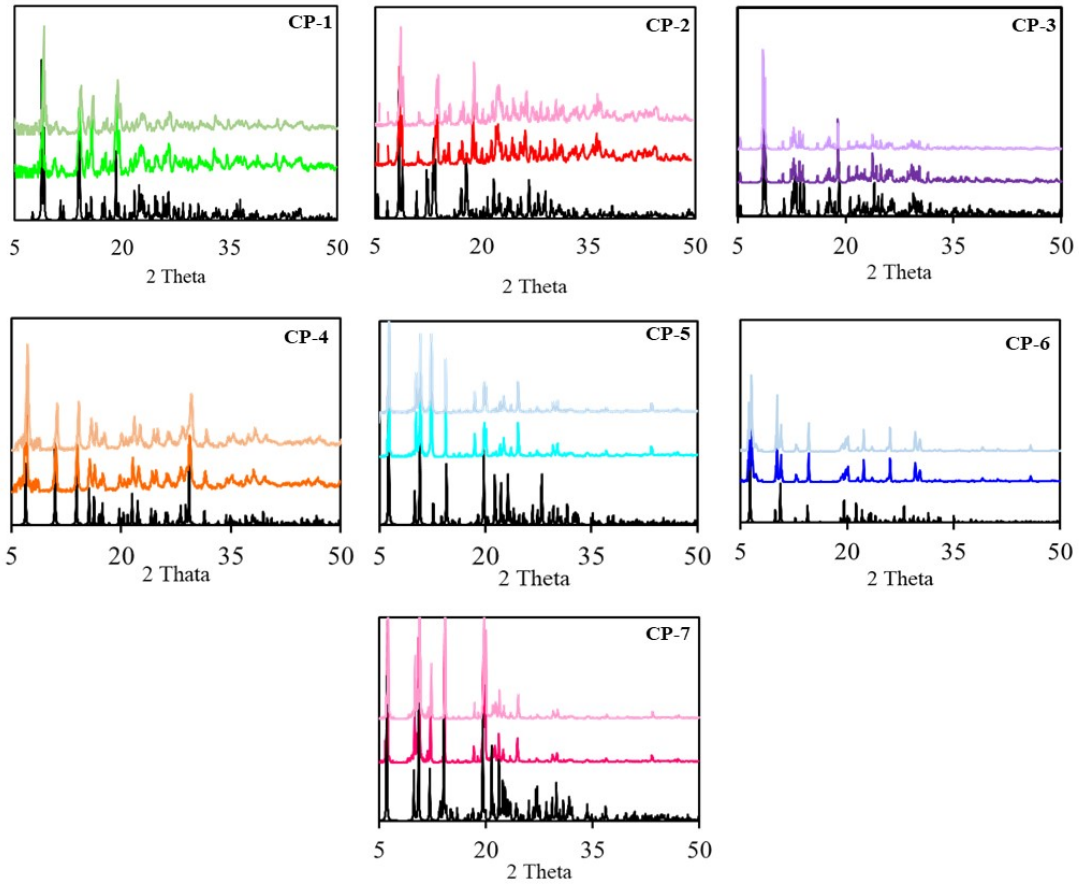

Figure S2: Comparison between the simulated powder X-ray diffraction patterns of the silver(I)-dithion coordination polymers (black pattern), experimental XRD patterns (bold colored pattern), and pale colored regenerated adsorbents after release of iodine patterns.

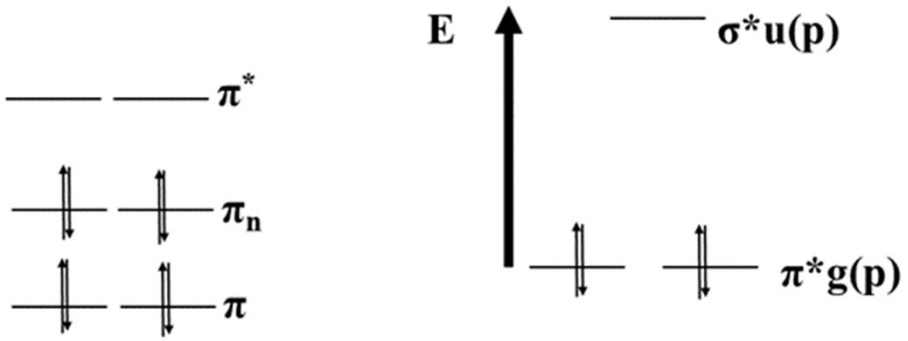

Figure S3: Simplified molecular orbital diagram of (a) SCN^- as a Lewis base, and (b) I_2 as a Lewis acid.

References:

(1) Sheldrick, G. M. SHELXT - Integrated Space-Group and Crystal-Structure Determination. *Acta Crystallogr. Sect. A Found. Crystallogr.* **2015**, *71* (1), 3–8.

(2) Sheldrick, G. M. Crystal Structure Refinement with SHELXL. *Acta Crystallogr. Sect. C Struct. Chem.* **2015**, *71* (1), 3–8.

(3) Ho, Y. S.; McKay, G. Pseudo-Second Order Model for Sorption Processes. *Process Biochem.* **1999**, *34* (5), 451–465.

(4) Özacar, M.; Şengil, I. A. A Kinetic Study of Metal Complex Dye Sorption onto Pine Sawdust. *Process Biochem.* **2005**, *40* (2), 565–572.

(5) Namasivayam, C.; Kavitha, D. Removal of Congo Red from Water by Adsorption onto Activated Carbon Prepared from Coir Pith, an Agricultural Solid Waste. *Dye. Pigment.* **2002**, *54* (1), 47–58.

(6) Langmuir, I. The Constitution and Fundamental Properties of Solids and Liquids. Part I. Solids. *J. Am. Chem. Soc.* **1916**, *38* (11), 2221–2295.

(7) Freundlich, H. M. F. Over the Adsorption in Solution. *Phys. chem.* **1906**, *57* (385471), 1100–1107.

(8) Tempkin, M.I. and Pyzhev, V. J. A. P. . Kinetics of Ammonia Synthesis on Promoted Iron Catalys. *Acta Phys. Chim. USSR.* **1940**, *12* (1), 327.